Long pulse D_2 and N_2 seeded discharges on the upper actively cooled tungsten divertor of WEST

T. Dittmar[a,*], T. Loarer[c], A. Drenik[b], C. Bourdelle[c], S. Brezinsek[a], C. Desgranges[c], D. Douai[c], N. Fedorczak[c], R. Guirlet[c], J. Gunn[c], O. Meyer[c], L. Laguardia[d], E. Tsitrone[c], and the WEST team[1]

[a] *Forschungszentrum Jülich GmbH, Institut für Energie- und Klimaforschung – Plasmaphysik, Partner of the Trilateral Euregio Cluster (TEC), 52425 Jülich, Germany*
[b] *Max-Planck-Institut für Plasmaphysik, 85748 Garching b. München, Germay*
[c] *CEAIRFM, EURATOM Assoc, F-13108 St Paul Les Durance, France*
[d] *Institute for Plasma Science and Technology, National Research Council of Italy, Milan, Italy*

Abstract

A series of L-mode discharges in upper single null configuration with more than 30 s duration were performed in the WEST tokamak with the strike line on actively cooled W-coated divertor components. This series of discharges accumulated 20 min of plasma and a strike point fluence of $\approx 2 \times 10^{25}\,\mathrm{m}^{-2}$ in 2 days of operation in attached conditions. The discharges showed good density control, no tungsten accumulation and an overall very benign thermal behaviour of the upper divertor. A subset of the discharges were seeded with nitrogen either in the divertor or midplane region to study plasma-wall interaction and associated ammonia formation in this weakly pumped scenario with all tungsten plasma facing components. While ammonia signals remained too weak for useful analysis, a strong dependence of nitrogen plasma penetration efficiency and residence time regarding the injection location was found. This hints towards a currently underestimated, plasma near nitrogen reservoir in these tokamak discharges in divertor configuration.

Keywords: tungsten divertor, WEST tokamak, long pulse operation, nitrogen seeding, ammonia formation

1. Introduction

The demands for high availability, low maintenance costs, and tritium safety considerations most certainly require that future fusion power plants will operate under steady-state conditions with a full metal environment for all plasma-facing components (PFCs). The necessity of high power exhaust rates and the intense plasma-wall interaction will require materials and engineering solutions at the edge e.g. for the current largest under-construction fusion experiment ITER or beyond the current manufacturing capabilities as expected for the future DEMO reactor. It is therefore necessary to test and evaluate developed full metal plasma-facing component solutions and operation regimes accessible with these components. The tokamak WEST thereby can provide an integrated platform for studying power exhaust physics and assessing power handling capabilities and lifetime of different components, including in particular the tungsten (W) high heat flux divertor technology envisaged for ITER [1, 2]. Another aspect is the study of long plasma pulses in an all W-PFC device. Therefore a series of long discharges with different heating schemes dedicated to study plasma-wall interaction and power exhaust of the upper cooled divertor of WEST were carried out to demonstrate the compatibility of plasma operation with W . This upper divertor is made of CuCrZr substrate coated with ≈15 µm of W [3].

Future reactor concepts most likely have to rely on impurity seeding to enhance radiative fraction beyond 95 % in order to cool in the plasma edge and thereby protect components from the plasma. Among the different gases tested in present fusion experimental devices, nitrogen (N_2) is a viable seeding candidate for the size and conditions in present

*Corresponding author
Email address: t.dittmar@fz-juelich.de (T. Dittmar)
[1] See the author list of http://west.cea.fr/WESTteam

day divertors. However, the rich chemistry of N_2, especially its tendency to form ammonia [4], provides challenges as ammonia interferes with the regeneration of cryo pumps and processes in future de-tritiation plants. Nevertheless, it is still foreseen in the ITER facility as radiator in the divertor due to its superb performance as shown in JET and ASDEX Upgrade (e.g. [5]). Therefore, some discharges were seeded with N_2 to study plasma-surface interaction (PSI) and ammonia formation in the full tungsten device WEST in order to improve the physics of ammonia production, decomposition and transport in a magnetically confined plasma device.

2. Discharge design and experimental setup

In order to achieve these goals, L-mode discharges in upper single null configuration (USN) were chosen in the WEST tokamak to study the performance and behaviour of the upper, actively cooled W coated divertor in long discharges. Global discharge parameters (toroidal field $B_T = 3.7$ T ,plasma current $I_p = 400$ kA, line averaged electron density $n_e \approx 3.3 \times 10^{19} m^{-2}$, primary gas filling: deuterium) and auxiliary heating conditions ($P_{lower\ hybrid} = 1.5 - 2.8$ MW) were designed to routinely achieve plasma duration longer than 30 s. In addition short pulses of ion cyclotron heating (ICRH) up to 0.6 MW was used to study plasma response.

To study the PSI and ammonia formation in this weakly pumped, cooled main PFC scenario some discharges were seeded with N_2. The seeding was started usually 10 s after the start of the discharge after establishing the discharge plateau. Moderate injection rates of 0.2 $Pa\,m^3 s^{-1}$ usually over 4 to 6 seconds were chosen in order not to perturb too strongly the plasma. While this seeding rate seems low, it is in the same order of magnitude as the D_2 gas flow rate during the plateau phase. The effect of different injection locations, either directly in the upper outer divertor region or at the movable midplane limiter were tested (compare fig 1 for the injection positions). It should be noted that the WEST upper divertor is not equipped with active pumping and all pumping was performed via turbo pumps connected to the midplane pump duct so that neutral particles had a relative long residence time in the divertor region which could effect the ammonia formation and decomposition.

The power exhaust capabilities and hot spot formation was observed with a set of infrared imaging systems covering different areas of the upper and lower divertor as well as the first wall [6, 7]. The total radiated power was reconstructed from a bolometric system measuring in the VUV-X band from 2 to 2000 Angstrom with a bolometric system (16 horizontal lines of sigth, 8 vertical). Although the bolometry tracks have been adapted to the divertor geometry, the overall detection system is still the same since the first plasma operated on Tore Supra [8]. The PSI in the upper divertor was observed with a fibre-coupled Princeton Instruments IsoPlane™ spectrometer system [9]. This system employs 36 lines of sight into the upper divertor in the visible spectral range. A spectral window of 360 nm to 420 nm was used to observe simultaneously deuterium as the main plasma constituent via D_δ and the expected intrinsic and extrinsic impurities W (as WI at 400.8 nm) , O_2 (OII, 397.3 nm) , and N_2 (NII, 399.5 nm). Plasma density, electron temperature and ion flux in the upper divertor region were measured with a set of embedded Langmuir probes [10]. In order to improve the reconstruction of plasma profiles at the target and the exact strike point position, a X-point height sweep was performed in most discharges.

The composition of the neutral gas in the vacuum vessel was analysed with a residual gas analyser (RGA) system located in the midplane pump duct. The system is comprised of two Pfeiffer quadrupol mass spectrometers (QMS). One recorded the whole available mass range in analogue mode as overview device and the second operated in MID mode with selected masses in the range of 1...28 amu in order to ameliorate the time resolution for the recording of the interesting species of the hydrogen, deuterium, methane, water and ammonia molecule fractions and isotopologues. The recorded mass spectrometer data was then analysed with a statistical algorithms [11] to de-convolute the overlapping contributions of these species in order to calculate the ammonia content and its H/D isotope fractions.

3. Results and discussion

A total of 40 pulses in L-mode with a plasma time of over 20 minutes and more than 800 seconds flat-top time were performed. In these pulses more than 2.3 GJ were injected into the plasma and a total fluence of $\approx 2 \times 10^{25}\,m^{-2}$ at the outer strike point location was achieved. The temperature at

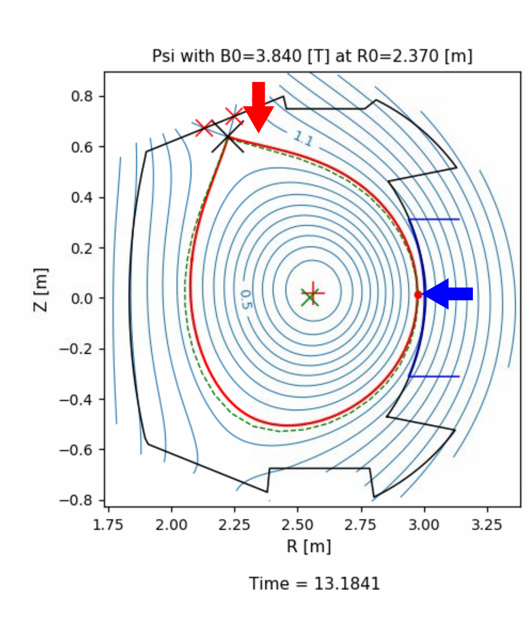

Figure 1: Typical magnetic configuration for the upper single null configuration used in this study. The arrows denote the approximate position of the gas inlets for the nitrogen seeding either located in the upper outer divertor region (red) and outer midplane (blue) region.

the outer strike point was $T_e \approx 10-15$ eV and an ion current of $J_{par} \approx 0.2$ A/cm^2 was achieved. Figure 2 shows time traces of the main plasma parameters for a typical discharge in the series. Despite the very weak pumping capabilities in the upper divertor the plasma shows good density control and about 30 s density flat-top is routinely achieved.

The discharge duration was limited ultimately by the available flux change in the central solenoid required to sustain a loop voltage of $V_{loop} \approx 0.2$ V which equilibrated from the used magnetic configuration, plasma parameters and lower hybrid auxiliary heating power. The discharges shows no sign of W or significant impurity accumulation and the radiated power fraction for the discharges stayed at quasi constant 55 % as calculated from bolometric reconstruction of the radiation profile. Observation of the cooled, upper divertor in the infrared shows no evidence for hot spot formation. The surface temperature increase of the upper divertor was below the detection limit of ~20K imposed by reflected infrared radiation from the lower, uncooled divertor which, despite not being in direct contact with the plasma, slowly heated up during the train of discharges ($\Delta T_{upper\,divertor} \approx 50$K).

The additional N_2 seeding had only little effect

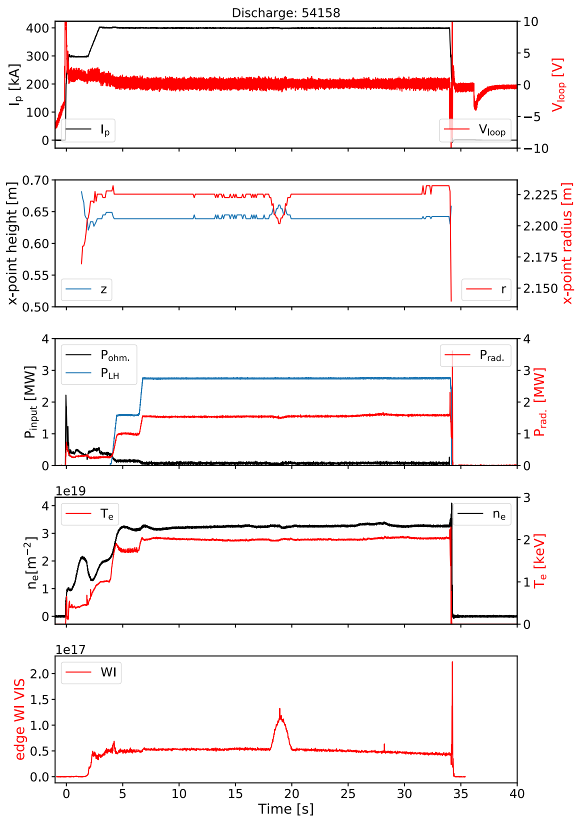

Figure 2: Time traces of different machine and plasma parameters for a typical unseeded discharge used for this analysis. The first panel shows the plasma current and the loop voltage. The second panel the z and r coordinates of the x-point which is sweeped around 18s into the discharge. The next panel shows the input power from the different heating systems and the reconstruction of the total radiated power from the bolometer signals. The fourth panel shows core plasma density and temperature and the last panel spectroscopic signals from optical emission spectroscopy from one line of sight close to the strike point in the outer part of the upper divertor. Note that while no W accumulation during the discharge is observed, the W I emmision is strongly dependend on the local plasma temperature and density in the observed volume. It is therefore very sensitive to the relative alignment of strike point position and observed line of sight and varies strongly with the shift of the plasma at $t \approx 17s$.

on the plasma operation: the global, absolute radiated power fraction for the discharges was only weakly affected by the N_2 injection. Nevertheless, the radiation pattern showed the pattern expected and desired for impurity seeding: moderately reduced radiation from the core region, meaning no additional core power losses but an improved edge radiation (here usually 20...30 % increase). Despite the increased edge radiation no effect on the divertor electron temperature was measurable in this attached plasma scenario. Furthermore, a slight increase in core electron temperature (T_e) and neutron production (from D(D,n)T reaction) observed both in the divertor and midplane seeded case hints at an improved confinement due to the N_2 seeding. While this is in line with results from other machines (e.g. [12]), further analysis of the plasma transport is required to understand the involved mechanisms and elucidate the specific role of the nitrogen seeding. QMS and spectroscopic observations of the nitrogen signals show only weak legacy effects from discharge to discharge for the applied N_2 seeding rate and amounts. The location of the N_2 injection, however, had significant influence: As can be seen by comparing the time traces in the figures 3a and 3b, a strong difference in the residence time of nitrogen was observed with variation of the N_2 injection location. In the case of N_2 being injected in the upper divertor, core and edge spectroscopy show a slower increase of nitrogen in core and edge and also very slow decay of visible nitrogen after the injection was stopped. Also, immediately after divertor seeded discharges a strong outgassing of N_2 is observed in the neutral gas diagnostics. This is in contrast to the seeding from the midplane location where core nitrogen signals show a much faster onset and decay behaviour and virtually no increase of the N_2 partial pressure after the end of the discharge is recorded. Altogether these findings hint at the presence of a reservoir of gaseous N_2 in the divertor region during the discharge.

Figure 4 shows the results of a deconvolution of the raw RGA data into the most probably partial pressures of ammonia, methane and water for the unseeded reference case and a divertor and midplane seeded discharge. While all cases show a significant post discharge raise in the the methane signal, no significant ammonia production is observed: For the reference discharge and midplane seeded discharges no ammonia signal is present. The weak post discharge ammonia increase could stem from

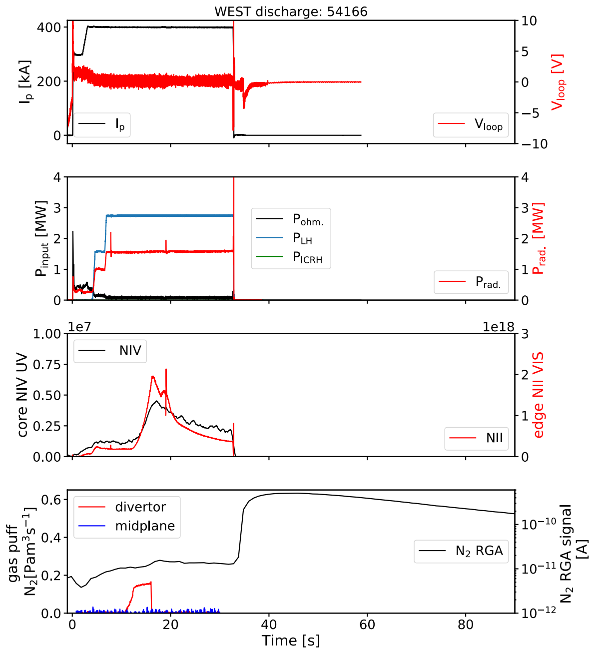

(a) gas puff in the outer divertor region

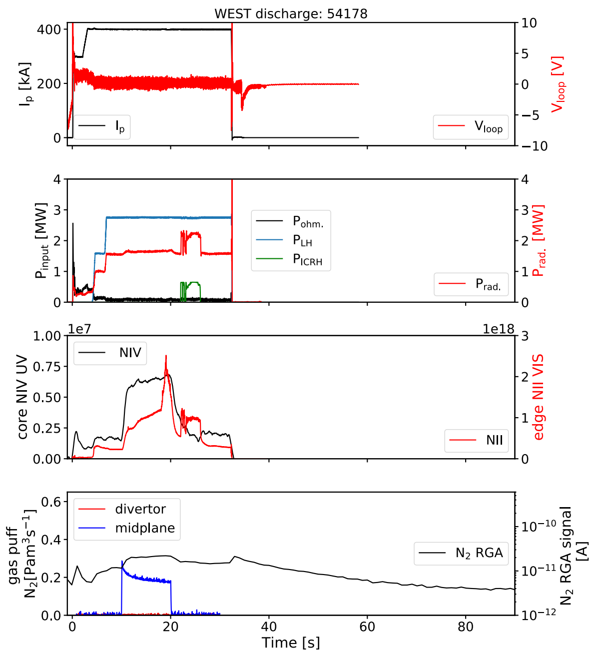

(b) gas puff in the outer midplane region

Figure 3: Time traces of plasma parameters and nitrogen related data for a) a divertor and b) a midplane seeded discharge. The first two panels show plasma parameters similar to fig. 2. Panel 3 shows optical emission spectral data for the core (NIV line) and the divertor (NII line). The last panel presents the N_2 seeding rates and the behaviour of the N_2 signal from residual gas analysis during the pulse and in the outgassing phase immediately after the discharge. The sudden increase of edge NI signals at $\approx$ 18 s is due to the strike point sweep. Note the slower decay of the plasma nitrogen content and the strong release of gaseous N_2 after the discharge in the case of the divertor seeding location.

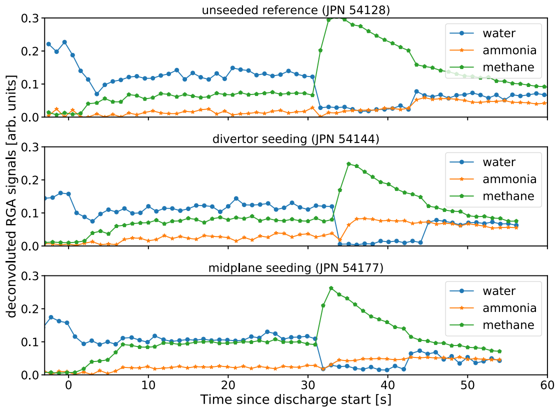

Figure 4: Result of the deconvolution regarding methane, water and ammonia content from the the raw mass spectrometer data for the two different seeding positions and an unseeded reference discharge.

ammonia produced in the plasma, nevertheless, it is more likely that it is an artefact in the deconvolution due to the strong methane signal in the post discharge gas release. On one hand this lack of detectable ammonia in the residual gas is shared in JET and ASDEX-U when the mass spectrometer is located far from the divertor [11, 13] and therefore expected. On the other hand, in these machines one contributor for a weak ammonia signals is the strong pumping in the divertor and therefore, in the weakly pumped upper divertor of WEST there was hope for a direct observation of ammonia in the neutral gas in the midplane pump duct. As small absolute amounts of injected N_2 were used in order to not disturb the discharge, the resulting ammonia production is obviously too low for direct detection.

4. Summary and Conclusions

In these series of attached L-mode long pulses the cooled upper divertor of WEST showed good power exhaust capabilities. No impurity accumulation or density issues were encountered and an integrated fluence of $\approx 2 \times 10^{25}\,\mathrm{m}^{-2}$ at the outer strike point was achieved. The discharges duration in this experimental session was limited to ≈ 30 s by the available magnetic flux to achieve the required 0.2 V loop voltage. Extrapolation show that an 1.2 MW increase of the power coupled from the lower hybrid heating system should reduce to loop voltage to 0.1 V. This will allow to reach discharge durations of above one minute. In the N_2 seeded discharges no direct quantification of the produced ammonia was possible and these experiments should be repeated with stronger N_2 seeding and additional mass spectrometry close to the divertor. The experiments varying the N_2 injection location between the divertor and the midplane showed a difference in the nitrogen plasma penetration and recycling. Furthermore these experiments showed a strong difference in post discharge N_2 release. This hints at a gaseous nitrogen reservoir in the divertor region and should be further studied as it will allow a better model for nitrogen transport in a tokamak.

Acknowledgements

This work has been carried out within the framework of the EUROfusion Consortium and has received funding from the Euratom research and training programme 2014-2018 under grant agreement No. 633053. The views and opinions expressed herein do not necessarily reflect those of the European Commission. This work was performed under EUROfusion WP PFC.

[1] C. Bourdelle, J. F. Artaud, V. Basiuk, M. Becoulet, S. Bremond, J. Bucalossi, H. Bufferand, G. Ciraolo, L. Colas, Y. Corre, X. Courtois, J. Decker, L. Delpech, P. Devynck, G. Dif-Pradalier, R. P. Doerner, D. Douai, R. Dumont, A. Ekedahl, N. Fedorczak, C. Fenzi, M. Firdaouss, J. Garcia, P. Ghendrih, C. Gil, G. Giruzzi, M. Goniche, C. Grisolia, A. Grosman, D. Guilhem, R. Guirlet, J. Gunn, P. Hennequin, J. Hillairet, T. Hoang, F. Imbeaux, I. Ivanova-Stanik, E. Joffrin, A. Kallenbach, J. Linke, T. Loarer, P. Lotte, P. Maget, Y. Marandet, M. L. Mayoral, O. Meyer, M. Missirlian, P. Mollard, P. Monier-Garbet, P. Moreau, E. Nardon, B. Pegourie, Y. Peysson, R. Sabot, F. Saint-Laurent, M. Schneider, J. M. Travere, E. Tsitrone, S. Vartanian, L. Vermare, M. Yoshida, R. Zagorski, WEST Physics Basis, Nuclear Fusion 55 (6) (2015) 063017. doi:10.1088/0029-5515/55/6/063017.

[2] J. Bucalossi, M. Missirlian, P. Moreau, F. Samaille, E. Tsitrone, D. van Houtte, T. Batal, C. Bourdelle, M. Chantant, Y. Corre, X. Courtois, L. Delpech, L. Doceul, D. Douai, H. Dougnac, F. Faisse, C. Fenzi, F. Ferlay, M. Firdaouss, L. Gargiulo, P. Garin, C. Gil, A. Grosman, D. Guilhem, J. Gunn, C. Hernandez, D. Keller, S. Larroque, F. Leroux, M. Lipa, P. Lotte, A. Martinez, O. Meyer, F. Micolon, P. Mollard, E. Nardon, R. Nouailletas, A. Pilia, M. Richou, S. Salasca, J. M. Travere, The WEST project: Testing ITER divertor high heat flux component technology in a steady state tokamak environment, Fusion Engineering and Design 89 (7-8) (2014) 907–912. doi:10.1016/j.fusengdes.2014.01.062.

[3] M. Richou, M. Missirlian, E. Tsitrone, J. Bucalossi, C. Desgranges, M. Firdaouss, D. Guilhem, H. Greuner, C. Hernandez, M. Lipa, G. Pintsuk, F. Samaille, The

WEST project: validation program for WEST tungsten coated plasma facing components, Physica Scripta T167 (2016) 014029. doi:10.1088/0031-8949/T167/1/014029.

[4] M. Oberkofler, D. Alegre, F. Aumayr, S. Brezinsek, T. Dittmar, K. Dobes, D. Douai, A. Drenik, M. Koeppen, U. Kruezi, C. Linsmeier, C. P. Lungu, G. Meisl, M. Mozetic, C. Porosnicu, V. Rohde, S. G. Romanelli, A. U. Team, J. E. Contributors, Plasma-wall interactions with nitrogen seeding in all-metal fusion devices: Formation of nitrides and ammonia, FUSION ENGINEERING AND DESIGN 98-99 (B) (2015) 1371–1374, 28th Symposium on Fusion Technology (SOFT), San Sebastian, SPAIN, SEP 29-OCT 03, 2014. doi:10.1016/j.fusengdes.2015.01.044.

[5] A. Kallenbach, R. Dux, J. C. Fuchs, R. Fischer, B. Geiger, L. Giannone, A. Herrmann, T. Lunt, V. Mertens, R. McDermott, R. Neu, T. Puetterich, S. Rathgeber, V. Rohde, K. Schmid, J. Schweinzer, W. Treutterer, Divertor power load feedback with nitrogen seeding in ASDEX Upgrade, Plasma Physics and Controlled Fusion 52 (5) (2010) 055002. doi:10.1088/0741-3335/52/5/055002.

[6] P. Moreau, J. Bucalossi, M. Missirlian, F. Samaille, X. Courtois, C. Gil, P. Lotte, O. Meyer, E. Nardon, R. Nouailletas, N. Ravenel, J. M. Travere, T. Alarcon, S. Antuschf, M. H. Aumeunier, P. Barjata, S. Belsare, J. M. Bernard, M. Bhandarkar, C. Bottereau, C. Bourdelle, S. Bremond, Y. Camenen, V. Chaudhari, C. Chavda, M. Chernyshova, F. Clairet, J. Colnel, T. Czarski, M. Choi, G. Colledni, Y. Corre, R. Daniel, D. Davis, R. Dejarnac, P. Devynck, J. Dhongde, D. Douai, D. Elbeze, A. Escarguel, C. Fenzi, W. Figacz, Z. Guangwu, J. C. Giacalone, R. Guirlet, J. Gunn, S. Hacquin, X. Hao, J. H. Harris, G. T. Hoang, M. Houry, F. Imbeaux, S. Jablonski, A. Jardin, H. Joshi, G. Kasprowicz, C. C. Klepper, E. Kowalska-Strzeciwilk, M. Kubkowska, A. Kumar, V. Kumar, P. Kumari, H. Laqua, A. Le-Luyer, W. Lee, M. Lewerentz, B. Lyu, P. Malard, L. Manenc, I. Mansuri, Y. Marandet, H. Masand, D. Mazon, D. Molina, G. Moureau, Y. Nam, H. Park, J. Y. Pascal, K. Patel, M. Patel, K. Pozniak, D. Radloff, S. Ranjan, C. Rapson, G. Raupp, M. Rieth, R. Sabot, B. Santraine, D. Sestac, M. Sharma, J. Shen, J. Signoret, J. Soni, A. Spring, P. Spuig, R. Sugandhi, W. Treuterrer, E. Tsitrone, S. Varshney, S. Vartanian, D. Volpe, F. D. Wang, A. Werner, G. Yun, W. Zabolotny, W. Zhao, Measurements and controls implementation for WEST, Fusion Engineering and Design 123 (2017) 1029–1032. doi:10.1016/j.fusengdes.2017.01.046.

[7] X. Courtois, M. H. Aumeunier, C. Balorin, K. Blanckaert, M. Houry, M. Jouve, P. Moreau, C. Pocheau, H. Roche, Design and status of the new WEST IR thermography system, Fusion Engineering and Design 136 (2018) 1499–1504. doi:10.1016/j.fusengdes.2018.05.042.

[8] K. F. MAST, J. C. VALLET, C. ANDELFINGER, P. BETZLER, H. KRAUS, G. SCHRAMM, A low-noise highly integrated bolometer array for absolute measurement of vuv and soft x-radiation, Review of Scientific Instruments 62 (3) (1991) 744–750. doi:10.1063/1.1142078.

[9] O. Meyer, J. C. Giacalone, A. Gouin, J. Y. Pascal, C. C. Klepper, N. Fedorczak, P. Lotte, E. A. Unterberg, D. T. Fehling, J. H. Harris, Visible spectroscopy diagnostics for tungsten source assessment in the WEST tokamak: First measurements, Review of Scientific Instruments 89 (10) (2018) 10D105. doi:10.1063/1.5035566.

[10] S. Antusch, J. Hoffmann, A. Klein, J. P. Gunn, M. Rieth, T. Weingaertner, Processing of complex near-net-shaped tungsten parts by PIM, NUCLEAR MATERIALS AND ENERGY 16 (2018) 71–75. doi:10.1016/j.nme.2018.05.023.

[11] A. Drenik, D. Alegre, S. Brezinsek, A. de Castro, U. Kruezi, G. Meisl, M. Mozetic, M. Oberkofler, M. Panjan, G. Primc, M. Resnik, V. Rohde, M. Seibt, F. L. Tabares, R. Zaplotnik, Detection of ammonia by residual gas analysis in AUG and JET, Fusion Engineering and Design 124 (2017) 239–243. doi:10.1016/j.fusengdes.2017.05.037.

[12] N. Bonanomi, P. Mantica, J. Citrin, C. Giroud, E. Lerche, C. Sozzi, D. Taylor, M. Tsalas, D. Van Eester, Effects of nitrogen seeding on core ion thermal transport in JET ILW L-mode plasmas, Nuclear Fusion 58 (2) (2018) 026028. doi:10.1088/1741-4326/aa9e7c.

[13] A. Drenik, L. Laguardia, R. McDermott, G. Meisl, R. Neu, M. Oberkofler, E. Pawelec, R. A. Pitts, T. Putterich, T. Reichbauer, V. Rohde, M. Seibt, G. De Temmerman, R. Zaplotnik, D. Aguiam, L. Aho-Mantila, C. Angioni, N. Arden, R. A. Parra, O. Asunta, M. de Baar, M. Balden, K. Behler, A. Bergmann, J. Bernardo, M. Bernert, M. Beurskens, A. Biancalani, R. Bilato, G. Birkenmeier, V. Bobkov, A. Bock, A. Bogomolov, T. Bolzonella, B. Boswirth, C. Bottereau, A. Bottino, H. van den Brand, S. Brezinsek, D. Brida, F. Brochard, C. Bruhn, J. Buchanan, A. Buhler, A. Burckhart, D. Cambon-Silva, Y. Camenen, P. Carvalho, G. Carrasco, C. Cazzaniga, M. Carr, D. Carralero, L. Casali, C. Castaldo, M. Cavedon, C. Challis, A. Chankin, I. Chapman, F. Clairet, I. Classen, S. Coda, R. Coelho, J. W. Coenen, L. Colas, G. Conway, S. Costea, D. P. Coster, G. Croci, G. Cseh, A. Czarnecka, O. D'Arcangelo, C. Day, R. Delogu, P. de Marne, S. Denk, P. Denner, M. Dibon, R. D'Inca, A. Di Siena, D. Douai, R. Drube, M. Dunne, B. P. Duval, R. Dux, T. Eich, S. Elgeti, K. Engelhardt, B. Erdos, I. Erofeev, B. Esposito, E. Fable, M. Faitsch, U. Fantz, H. Faugel, F. Felici, S. Fietz, A. Figueredo, R. Fischer, O. Ford, L. Frassinetti, S. Freethy, M. Froeschle, G. Fuchert, J. C. Fuchs, H. Fuenfgelder, K. Galazka, J. Galdon-Quiroga, A. Gallo, Y. Gao, S. Garavaglia, M. Garcia-Munoz, B. Geiger, C. Cianfarani, L. Giannone, E. Giovannozzi, C. Gleason-Gonzalez, S. Gloeggler, M. Gobbin, T. Goerler, T. Goodman, G. Gorini, D. Gradic, A. Graeter, G. Granucci, H. Greuner, M. Griener, M. Groth, A. Gude, S. Guenter, L. Guimarais, G. Haas, A. H. Hakola, C. Ham, T. Happel, J. Harrison, D. Hatch, V. Hauer, T. Hayward, B. Heinemann, S. Heinzel, T. Hellsten, S. Henderson, P. Hennequin, A. Herrmann, E. Heyn, F. Hitzler, J. Hobirk, M. Hoelzl, T. Hoeschen, J. H. Holm, C. Hopf, F. Hoppe, L. Horvath, A. Houben, A. Huber, V. Igochine, T. Ilkei, I. Ivanova-Stanik, W. Jacob, A. S. Jacobsen, J. Jacquot, F. Janky, A. Jardin, F. Jaulmes, F. Jenko, T. Jensen, E. Joffrin, C. Kaesemann, A. Kallenbach, S. Kalvin, M. Kantor, A. Kappatou, O. Kardaun, J. Karhunen, S. Kasilov, W. Kernbichler, D. Kim, S. Kimmig, A. Kirk, H. J. Klingshirn, F. Koch, G. Kocsis, A. Koehn, M. Kraus, K. Krieger, A. Krivska, A. Kraemer-Flecken, T. Kurki-Suonio, B. Kurzan, K. Lackner, F. Laggner,

P. T. Lang, P. Lauber, N. Lazanyi, A. Lazaros, A. Lebschy, L. Li, M. Li, Y. Liang, B. Lipschultz, Y. Liu, A. Lohs, N. C. Luhmann, T. Lunt, A. Lyssoivan, J. Madsen, H. Maier, O. Maj, J. Mailloux, E. Maljaars, P. Manas, A. Mancini, A. Manhard, M. E. Manso, P. Mantica, M. Mantsinen, P. Manz, M. Maraschek, C. Martens, P. Martin, L. Marrelli, A. Martitsch, S. Mastrostefano, A. Mayer, M. Mayer, D. Mazon, P. J. McCarthy, H. Meister, A. Medvedeva, P. Merkel, R. Merkel, A. Merle, V. Mertens, D. Meshcheriakov, H. Meyer, O. Meyer, J. Miettunen, D. Milanesio, F. Mink, A. Mlynek, F. Monaco, C. Moon, R. Nazikian, A. Nemes-Czopf, G. Neu, R. Neu, A. H. Nielsen, S. K. Nielsen, V. Nikolaeva, M. Nocente, J. M. Noterdaeme, S. Nowak, M. Oberparleiter, R. Ochoukov, T. Odstrcil, J. Olsen, F. Orain, F. Palermo, G. Papp, I. P. Perez, G. Pautasso, F. Enzel, P. Petersson, J. Pinzon, P. Piovesan, C. Piron, B. Plaum, B. Ploeckl, V. Plyusnin, G. Pokol, E. Poli, L. Porte, S. Potzel, D. Prisiazhniuk, M. Ramisch, C. Rapson, J. Rasmussen, G. Raupp, D. Refy, M. Reich, F. Reimold, T. Ribeiro, R. Riedl, D. Rittich, G. Rocchi, M. Rodriguez-Ramos, V. Rohde, A. Ross, M. Rott, M. Rubel, D. Ryan, F. Ryter, S. Saarelma, M. Salewski, A. Salmi, L. Sanchis-Sanchez, G. Santos, J. Santos, O. Sauter, A. Scarabosio, G. Schall, K. Schmid, O. Schmitz, P. A. Schneider, M. Schneller, R. Schrittwieser, M. Schubert, T. Schwarz-Selinger, J. Schweinzer, B. Scott, T. Sehmer, M. Sertoli, A. Shabbir, A. Shalpegin, L. Shao, S. Sharapov, M. Siccinio, B. Sieglin, A. Sigalov, A. Silva, C. Silva, P. Simon, J. Simpson, A. Snicker, C. Sommariva, C. Sozzi, M. Spolaore, M. Stejner, J. Stober, F. Stobbe, U. Stroth, E. Strumberger, G. Suarez, K. Sugiyama, H. J. Sun, W. Suttrop, T. Szepesi, B. Tal, T. Tala, G. Tardini, M. Tardocchi, D. Terranova, W. Tierens, D. Told, O. Tudisco, G. Trevisan, W. Treutterer, E. Trier, M. Tripsky, M. Valisa, M. Valovic, B. Vanovac, P. Varela, S. Varoutis, G. Verdoolaege, D. Vezinet, N. Vianello, J. Vicente, T. Vierle, E. Viezzer, U. Toussaint, D. Wagner, N. Wang, X. Wang, M. Weidl, M. Weiland, A. E. White, M. Willensdorfer, B. Wiringer, M. Wischmeier, R. Wolf, E. Wolfrum, L. Xiang, Q. Yang, Z. Yang, Q. Yu, R. Zagorski, I. Zammuto, D. Zarzoso, W. Zhang, M. Zeeland, T. Zehetbauer, M. Zilker, S. Zoletnik, H. Zohm, Evolution of nitrogen concentration and ammonia production in N-2-seeded H-mode discharges at ASDEX Upgrade, Nuclear Fusion 59 (4) (2019) 046010. doi:10.1088/1741-4326/aafe23.